


MicroRNA-499 Suppresses the Growth of Hepatocellular Carcinoma by Downregulating Astrocyte Elevated Gene-1

Technology in Cancer Research & Treatment
Volume 19: 1-9
© The Author(s) 2020
Article reuse guidelines:
sagepub.com/journals-permissions
DOI: 10.1177/1533033820920253
journals.sagepub.com/home/tct


Jing Wang, MD¹, Jia Li, MD¹, Liping Chen, MD², Zhenyu Fan, MD², and Jilin Cheng, MD² 

Abstract

The aim of this study is to investigate the role of microRNA-499 (miR-499) in hepatocellular carcinoma tumor growth and the underlying molecular mechanisms. The expression of miR-499 was significantly decreased in hepatocellular carcinoma tissues compared with that in adjacent normal tissues. Furthermore, miR-499 overexpression in HEPG2 cell was related to the tumor growth in nude mice xenograft models. Likewise, miR-499 mimic or inhibitor decreased or accelerated cell proliferation, respectively. Mechanistically, miR-499 directly targeted the 3'- untranslated region of astrocyte elevated gene-1 and downregulate astrocyte elevated gene-1 expression. Restoration of astrocyte elevated gene-1 expression in hepatocellular carcinoma cells reversed the inhibitory effect of miR-499 on cell growth. In addition, astrocyte elevated gene-1 and miR-499 expression were inversely correlated in human and mice hepatocellular carcinoma tissues. Our study identified miR-499 as a tumor-suppressive miR in hepatocellular carcinoma, thus providing a candidate therapeutic target for the future diagnosis or treatment of hepatocellular carcinoma.

Keywords

miR-499, astrocyte elevated gene-1 (AEG-1), hepatocellular carcinoma cells, cell growth, targeted regulation

Abbreviations

AEG-1, astrocyte-elevated gene-1; CCK-8, cell counting-8 kit; cDNA, complementary DNA; DMEM, Dulbecco's modified eagle medium; FBS, fetal bovine serum; HCC, hepatocellular carcinoma; mRNA, messenger RNA; miRNA, microRNA; PCR, polymerase chain reaction; PVDF, polyvinylidene difluoride

Received: September 14, 2019; Revised: March 02, 2020; Accepted: March 26, 2020.

Background

Hepatocellular carcinoma (HCC) is one of the most common malignant tumor with high mortality worldwide.^{1,2} Hepatocellular carcinoma is prone to occur early metastasis and often has a high recurrence rate.^{3,4} Surgical resection is considered to be the main therapeutic treatment for early patients with HCC, but the prognosis is still poor.⁵ In addition, the efficacy of combination therapy for patients with end-stage cancer, including post-operative molecular targeting therapy, radiotherapy, and immunotherapy, is also unsatisfactory.^{6,7} Till now, the detailed pathogenesis of HCC progression is still poorly understood. The molecular mechanisms of HCC remain to be investigated in order to develop potential therapeutic targets for patients with HCC.

Previous research studies have identified a variety of HCC-related genes involved in liver cancer progression, such as

defective kernel (DEK), cyclin D1, and insulin-like growth factor II.⁸ MicroRNAs (miRNAs), which are noncoding RNAs composed of 18 to 24 nucleotides, were reported to regulate the expression of their target genes in posttranscriptional level, thereby participating in various biological processes, including cell proliferation, apoptosis, migration, and invasion.^{9,10}

¹ Department of Hepatology, Tianjin Second People's Hospital, Tianjin Liver Disease Research Institute, Tianjin, China

² Department of Gastroenterology, Shanghai Public Health Clinical Center, Shanghai, China

Corresponding Author:

Jilin Cheng, Department of Gastroenterology, Shanghai Public Health Clinical Center, 2901 Caolang Road, Jinshan District, Shanghai 201508, China.
Email: chengjlll@163.com



Mechanistically, miRNAs impair messenger RNA (mRNA) degradation or translation by binding to the 3'-untranslated region (UTR) of target genes, leading to mRNA destabilization and protein translational inhibition.¹¹ The progression of HCC is also found to be regulated by various kinds of miRNAs.¹²⁻¹⁶ Particularly, miRNA-499 was found to act as a biological indicator for the prognosis of HCC.¹⁷ A previous work showed that downregulation of miR-499 promoted the HCC cell proliferation by histone deacetylases (HDAC1-3), suggesting that miR-499 may serve as a tumor suppressor.¹⁸ However, the detailed molecular mechanisms of miR-499 in modulating HCC development are still elusive.

Astrocyte-elevated gene-1 (AEG-1) is a typical oncogene which promotes tumor growth, angiogenesis, metastasis, and drug resistance.¹⁹ Astrocyte-elevated gene-1 is found to be highly expressed in many kinds of cancers, including ovarian cancer, breast cancer, esophageal squamous cell carcinoma, gastric cancer, colorectal cancer, non-small cell lung cancer, neuroblastoma, and kidney cancer.^{20,21} Phosphatidylinositol 3-kinase (PI3K)/Akt, mitogen-activated protein kinase, Wnt/ β -catenin, and nuclear factor- κ B pathways were reported to promote the transcription of AEG-1 in cancer cells.²¹⁻²³ In HCC cells, high AEG-1 expression led to the enhanced cell proliferation and invasion,^{21,24} suggesting the pathogenic role of AEG-1 in HCC. Nevertheless, how AEG-1 expression is regulated in HCC is still unclear. In the present study, we investigated the role of miR-499 and its functional target AEG-1 in HCC development.

Material and Methods

Materials

Oligonucleotides of miR-499 mimics, miR-499 inhibitor, negative controls (Ct), and small interfering RNA of AEG-1 were synthesized by Genepharma Co, Ltd (Shanghai, China). Astrocyte-elevated gene-1 overexpression plasmid (pCDNA3.1) and empty vector were also constructed by Shanghai GenePharma (Shanghai, China). Luciferase reporter plasmids containing the wild type seed regions of miR-499 in the 3'-UTR of AEG-1 were chemically synthesized by GenePharma. Bovine serum albumin was purchased from Sigma-Aldrich (St. Louis, Missouri). Dulbecco's modified eagle medium (DMEM) and fetal bovine serum (FBS) were obtained from Gibco BRL Life Technologies Inc (Carlsbad, California). BCA Protein Assay Kit, polyvinylidene difluoride (PVDF) membrane, and horseradish peroxidase-conjugated anti-rabbit IgG were provided by Thermo Fisher Scientific (Rockford, Illinois). TRIZOL reagent was purchased by Invitrogen (Carlsbad, California). Cell Counting-8 Kit (CCK-8) was obtained from Dojindo Laboratories (Tokyo, Japan). Penicillin and streptomycin were purchased from Beyotime Biotechnology (Shanghai, China).

Patient Samples

Patient samples were obtained from the Shanghai Public Health Clinical Center. The 15 samples of HCC and paired adjacent

liver tissues were obtained from patients during the operation. This study was approved by the Shanghai Public Health Clinical Center Ethical Committee (approval no. SPHE-20180517a). All patients provided written informed consent prior to enrollment in the study. All tissue specimens were stored at -80°C until use.

Cell Culture and Treatment

Cell line and vectors construction. Human HCC cell lines HEPG2 were provided by Chinese Academy of Sciences (Shanghai, China) and cultured in DMEM supplemented with 10% FBS (Gibco), penicillin (100 U/mL), and streptomycin (100 $\mu\text{g}/\text{mL}$). Cells were cultured and maintained at 37°C in a humidified atmosphere of 5% CO_2 incubator.

Cell transfection. To investigate the precise significance of miR-499 in HCC, miR-499 mimics, miR-499 inhibitor, and their negative control nucleotides were transiently transfected into HEPG2 cells. Based on the different treatment methods, HEPG2 cells were divided into 4 groups: the control mimic group (Ct mimic); the miR-499 mimic group (miR-499 mimic); the control inhibitor group (Ct inhibitor); and the miR-499 inhibitor group (miR-499 inhibitor). Cells were plated into 6-well plate with 70% to 80% confluence 24 hours prior to transfection. The oligonucleotides (50 pmol/mL) and vectors (2 μg) were transfected into HEPG2 cells using Lipofectamine 2000 (Invitrogen) according to the manufacturer's instructions. After 48-hour transfection, the subsequent experiment was carried out.

Dual-luciferase reporter assay. For the dual-luciferase reporter assay, cells were plated into 24-wells plates before transfection. Cells were co-transfected with miR-499 mimic or miR-499 inhibitor and luciferase reporter recombinant plasmid (containing an AEG-1 3'-UTR construct) using lipofectamine2000 reagent. Following cultivation for 48 hours, the cells were harvested, and luciferase activity was determined using a dual-luciferase reporter assay system based on the manufacturer's instructions. Renilla luciferase activity was used as an internal reference for Firefly luciferase activity.

Cellular proliferation assay. The CCK-8 assay was performed to assess cell proliferation. Briefly, transfected HEPG2 cells were seeded in 96-wells plate at a density of 5000 cells/well, and the cells were washed 3 times after incubation at 37°C overnight. Serum-free medium was added into each well, and cell proliferation was measured at 24, 48, and 72 hours. Subsequently, 10 μL of CCK-8 reagent per well was added and incubated for 1 hour at 37°C , the absorption value was measured at 450 nm following the manufacturer's protocol.

Preparation of cell lysates and Western blot assay. The expression of AEG-1 in transfected HEPG2 (mimic and inhibitor) was confirmed by Western blot. Cultured cell lysates were prepared by lysis buffer supplemented with a protease inhibitor cocktail. The protein concentration of each sample was determined with

the BCA Kit (Beyotime, Beijing, China). Protein samples were separated by sodium dodecyl sulphate–polyacrylamide gel electrophoresis and subsequently transferred to PVDF membrane for 120 minutes at 300 mA. After washing 3 times in TBST for 5 minutes, the membranes were incubated with the primary antibodies (AEG-1 and GAPDH) at 4°C overnight and the corresponding second antibodies were added for 1 hour at room temperature. Then immunoreactive bands were visualized by automatic chemiluminescence image analysis system (Tanon 5200 Multi, Shanghai, China).

Nude Mice Xenograft Studies

Female BALB/c nude mice (4–6 weeks of age; Vital River Laboratory Animal Technology Co Ltd, Beijing, China) were housed in a specific pathogen-free animal facility with controlled light (12-hour light/dark cycles), temperature, and humidity, with standard chow diet and water available. All the experimental procedures involving animals were approved by the Institutional Animal Care and Use Committee of Shanghai Public Health Clinical Center.

Subcutaneous xenograft models were established in the flanks of athymic nude mice using a density of 5×10^5 HEPG2 cells. For long-term studies of miR-499 on liver tumor development, nude mice with 4 to 6 weeks of age were subcutaneously injected with HEPG2-miR-499 (transfected with miR-499 expression vectors) and detected for 22 days. Injection of HEPG2 cell in a group of age-matched mice served as controls. Xenografts tumor volume in 2 groups were measured at 8, 13, 17, and 22 days with a caliper and calculated using the following formula: length \times width \times width/2. For an assessment of the tumor weight, groups of HEPG2-miR-499 or HEPG2 injected nude mice were sacrificed 22 days after the fourth injection of miRNA. Mice were sacrificed by cervical dislocation under anesthesia with ether and the xenograft tumor tissue was explanted, isolated, and analyzed after 22 days for examination. For survival rate assays, 5×10^5 HEPG2 and HEPG2-miR-499 cells were subcutaneously xenotransplanted in the flanks of nude mice and followed for 5 weeks. All experiments were performed with at least 8 mice in each group, and all of the experiments were repeated 3 times. After transfected with miR-499 overexpression vector, or control, HEPG2 cells were injected into nude mice and subcutaneously growth of HEPG2 in nude mice were detected by measuring.

Real-Time Polymerase Chain Reaction Analysis

Total RNA of human HCC and cells was extracted with Trizol (Invitrogen) according to standard procedures. The OD260/280 value of the extracted RNA was detected with an ultraviolet spectrophotometer, and the RNA concentration was calculated. Then, reverse transcription of complementary DNA (cDNA) was performed following the instructions of the kit by the manufacturer's instructions (Takara, Shiga, Japan). Quantification of mRNA levels was conducted in the

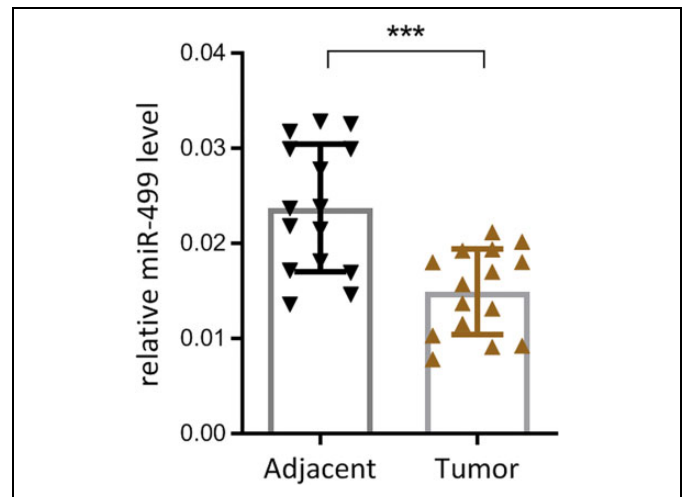


Figure 1. The expression level of microRNA-499 (miR-499) in 15 hepatocellular carcinoma tissues is downregulated compared to the adjacent liver tissues. Expression of miR-499 was analyzed by real-time polymerase chain reaction (PCR) and normalized against an endogenous control (U6 RNA). Data are mean \pm standard deviation, *** $P < .001$.

ABI PRISM 7500 Sequence Detection System (Applied Biosystems, Foster City, California) following the manufacturer's protocols. The designed primers were synthesized by Shanghai Sangon Biotech (Shanghai, China): miR-499, F, 5'-TAGAAGCTTGTGTCCAGCTGCACAAGGTA-3'; R, 5'-TATCTCGAGTGTCTCCATCACCACCACCA-3'; AEG-1, F, 5'-TTGAAGTGGCTGAGGGTGAA-3'; R, 5'-TACGCTGCTGTCGTTTCTCT-3'. The transcriptional levels of genes including AEG-1 and β -actin were examined. Data were analyzed by the $2^{-\Delta\Delta Ct}$ methods, and cDNAs were normalized to equal amounts using primers against β -actin.

Statistical Analysis

Results were expressed as mean \pm standard deviation. The differences between groups were analyzed by Brown-Forsythe test and, if appropriate, by 1-way analysis of variance. A P value of less than .05 was considered significant. All assays were repeated for 3 times.

Results

Reduced miRNA-499 Expression in HCC Tissues

First, we analyzed miR-499 expression in 15 HCC tumor tissues and the paired-adjacent non-tumorous tissues by real-time polymerase chain reaction (PCR). The results showed that the expression of miR-499 in HCC tumor tissues was significantly lower as compared to that in the matched adjacent liver tissues ($P < .001$; Figure 1). Therefore, we hypothesized that miRNA-499 was involved in modulating HCC progression.

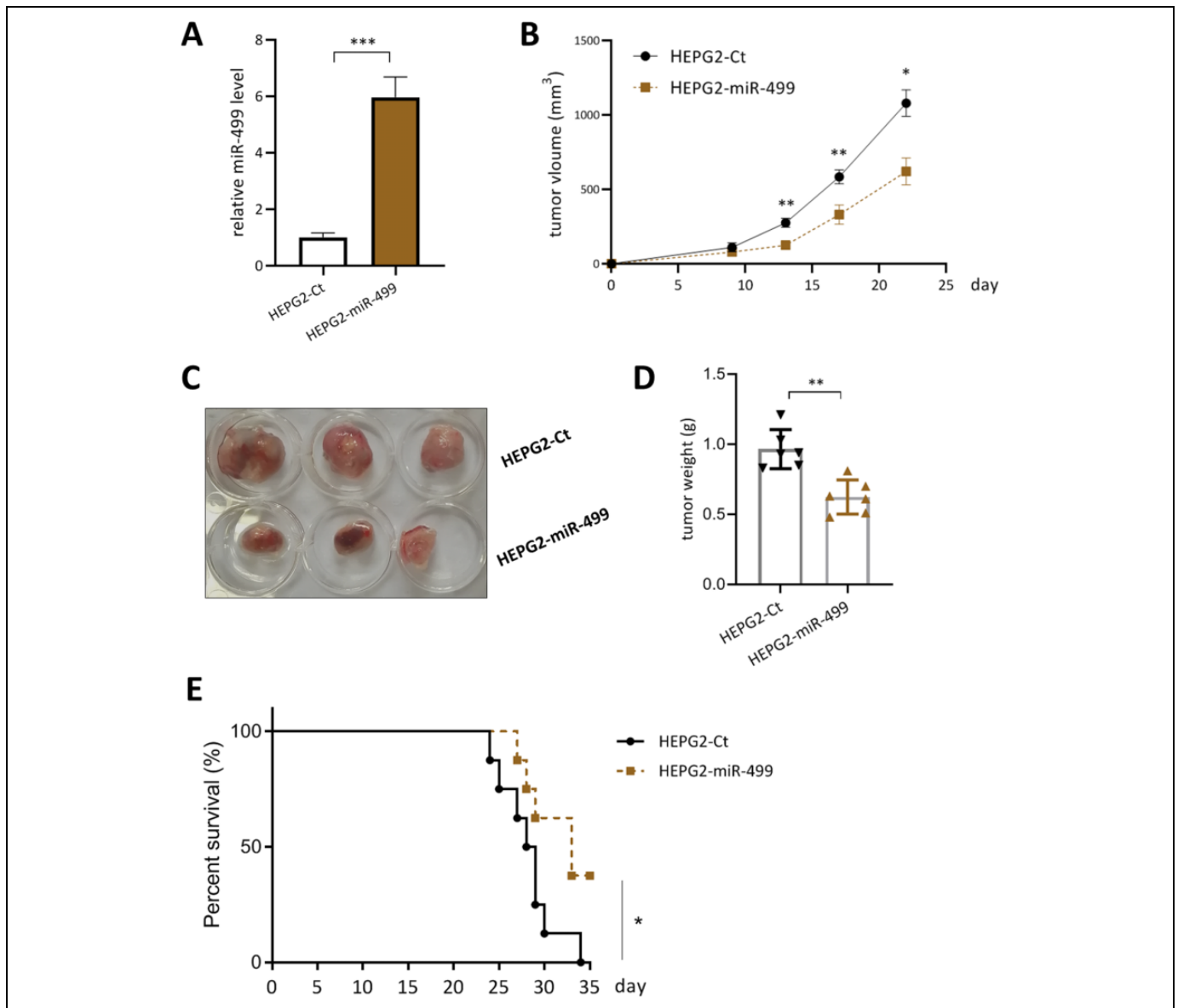


Figure 2. MicroRNA-499 (miR-499) overexpression suppresses the xenograft tumor growth of subcutaneous nude mice. A, miR-499 expression efficiency was measured after overexpression of miR-499 in HEPG2 cells. MicroRNA-499 expression level in HEPG2 cells transfected with miR-499 mimic was verified by real time-PCR. Data are from 3 independent experiments (mean \pm SD). *** $P < .001$. Analysis of the xenograft tumors generated after injection with HEPG2 cells with miR-499 overexpression plasmids in nude mice, and HEPG2 cells as control. B, Comparative analysis of nude mice tumor growth curve in 2 groups at the indicated time. Data are mean \pm SD; * $P < .05$; ** $P < .01$. C, Representative images of hepatoma xenograft tumors in the HEPG2-Ct (upper panel) and HEPG2-miR-499 (lower panel) nude mice groups at day 22. D, Measure of tumor weight in 2 groups at the end of the study. Data are mean \pm SD; ** $P < .01$. E, The overall survival rate of the HCC nude mice between HEPG2-Ct and HEPG2-miR-499 groups. The survival rate in nude mice was evaluated by Kaplan–Meier via the log-rank test. Data are mean \pm SD; * $P < .05$; $N = 8$. HCC indicates hepatocellular carcinoma; PCR, polymerase chain reaction; SD, standard deviation.

MicroRNA-499 Overexpression Reduced HCC Tumor Growth in Mice

In order to further evaluate the biological functions of miR-499 on liver tumor development, we employed a subcutaneous tumor xenografted model in nude mice. To this end, HEPG2 cells were stably overexpressed with miR-499 (Figure 2A) and then were subcutaneously injected into mice. Tumor volume

was measured every 5 days postinjection. The results showed that compared to the control group (HEPG2-Ct), tumor growth rate in miR-499 overexpression group (HEPG2-miR-499) was significantly decreased (Figure 2B). Mice were sacrificed on 22 days and tumors tissues were isolated and photographed, we found that the average volume of the tumor was decreased significantly in miR-499 overexpression group (Figure 2C).

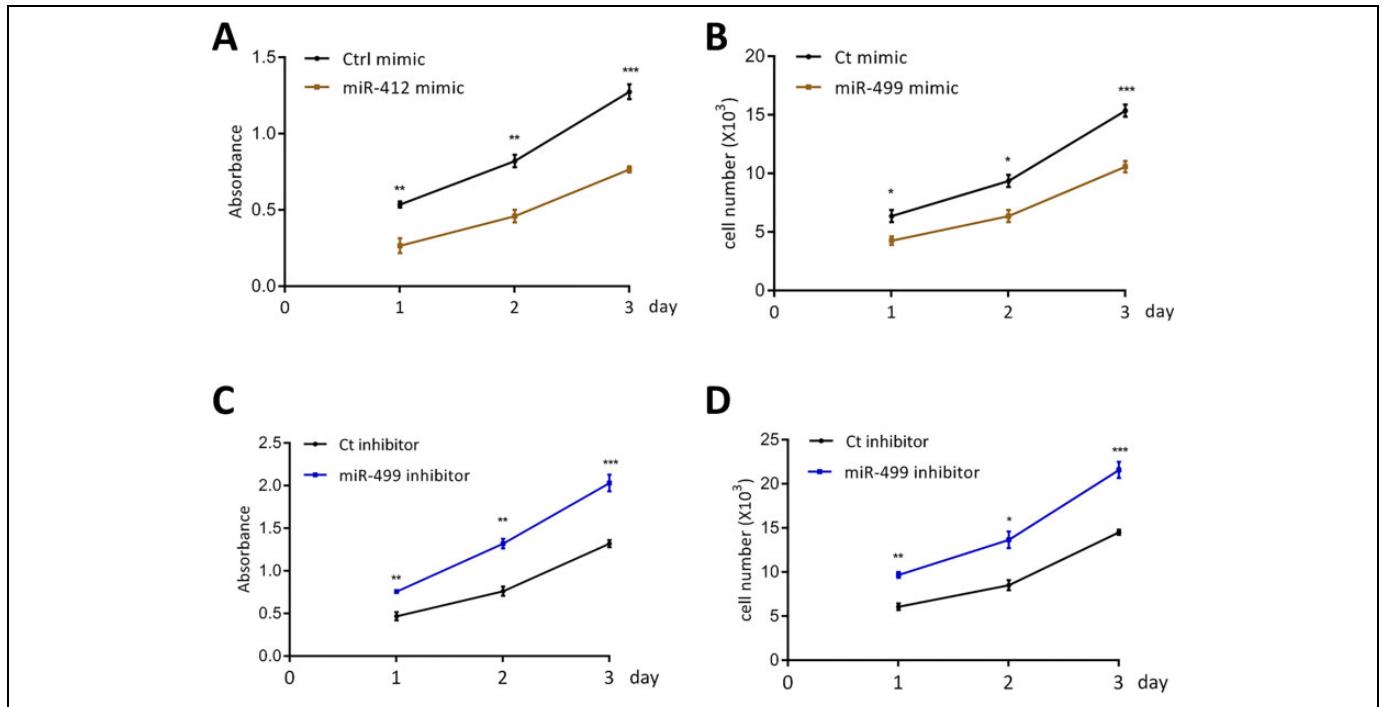


Figure 3. MicroRNA-499 (miR-499) inhibits the growth of HEPG2 cells. HEPG2 cells were transiently transfected with miR-499 mimics (A, C) or miR-499 inhibitor (C, D) for 48 hours. The cell proliferation was measured for 0, 24, 48, and 72 hours by CCK-8 assay (A, C) and counting (B, D). * $P < .05$; ** $P < .01$, *** $P < .001$ versus Ct group. CCK-8 indicates cell counting-8 kit.

In addition, the tumor weight in HEPG2-miR-499 group (0.623 ± 0.21 g) was significantly lower than that in the control group (0.962 ± 0.19 g) on day 22 ($P < .01$; Figure 2D). Moreover, survival analysis revealed that miR-499 overexpression significantly improved overall survival in HEPG2 tumor-bearing mice (Figure 2E). These data demonstrated that miR-499 served as an antitumor miR in HCC.

MicroRNA-499 Suppresses the Growth of HEPG2 Cells

To further explore the biological function of miR-499 *in vitro*, we transfected miR-499 mimic or miR-499 inhibitor into HEPG2 cells. The transfection efficiency was confirmed by real-time PCR analysis, and the miR-499 expression level increased with miR-499 mimic and decreased with miR-499 inhibitor (data not shown). We then examined the effect of miR-499 on cell proliferation using CCK-8 assay. As shown in Figure 3A and C, miR-499 mimic significantly reduced the proliferation of HEPG2 cells 48 hours post-transfection, whereas miR-499 inhibition by miR-499 inhibitor markedly promoted cell proliferation. Similarly, the number of HEPG2 cells was significant reduced after miR-499 mimic transfection, while miR-499 inhibition significantly increased the number of HEPG2 cells (Figure 3B and D). Taken together, these data showed that miR-499 could cause growth retardation of HEPG2 cells.

MicroRNA-499 Targets the 3'-UTR of AEG-1 to Inhibit AEG-1 Expression

To elucidate the underlying mechanism by which miR-499 inhibits cell growth, bioinformatics analysis was performed to search for the potential miR-499 target genes. Using the online miRNA target gene prediction tool TargetScan (<http://www.targetscan.org/>), an miR-499-binding site was observed in the 3'-UTR of AEG-1 (Figure 4A). To investigate whether miR-499 directly regulates AEG-1 expression, we evaluated the effect of miR-499 overexpression or inhibition on AEG-1 expression by real-time PCR and Western blot analysis. As shown in Figure 4B and C, transfection with miR-499 mimic significantly decreased both the mRNA and protein levels of AEG-1, whereas miR-499 inhibitor increased their levels. To further verify whether miR-499 directly targets the 3'-UTR of AEG-1, we performed dual-luciferase reporter assays by inserting an AEG-1 3'-UTR into a luciferase reporter vector. As shown in Figure 4D, miR-499 mimic significantly inhibited the luciferase activity, whereas miR-499 inhibition increased the luciferase activity.

Next, we looked at the effect of AEG-1 on the proliferation of HEPG2 cells by CCK-8 assay. Restored AEG-1 expression reversed the suppressive effect of miR-499 mimic on the proliferation of HEPG2 cells (Figure 4E). On the other hand, AEG-1 silencing reduced cell proliferation in miR-499 inhibitor-transfected HEPG2 cells (Figure 4F). The efficiency

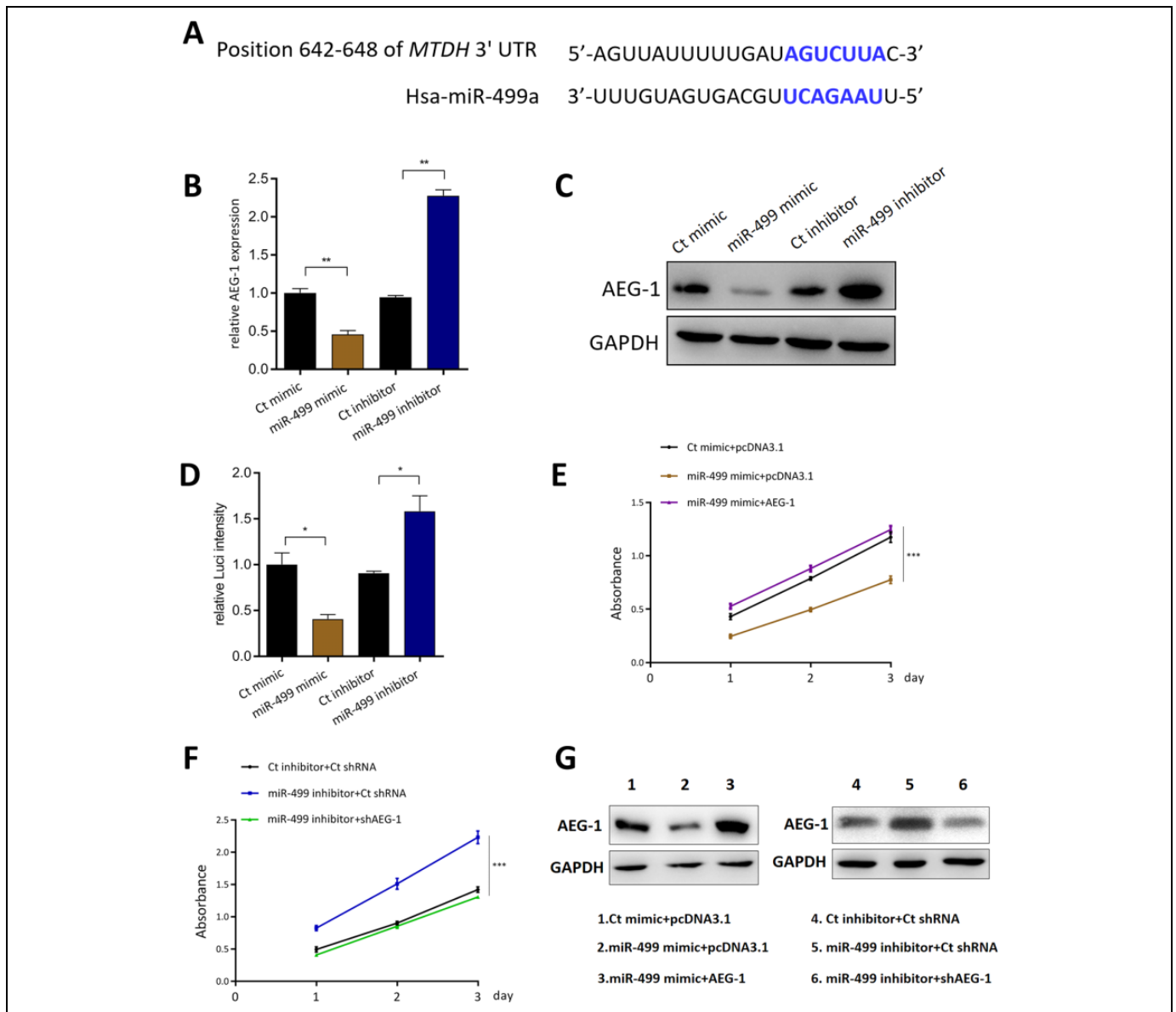


Figure 4. Astrocyte-elevated gene-1 (AEG-1) is a direct target of microRNA-499 (miR-499) in HEPG2. MicroRNA-499 binds to AEG-1 3'-UTR using the prediction of Targetscan online software. A, Schematic diagram of the miR-499 putative binding site in the 3'-UTR of AEG-1. Cells were co-transfected with wild-type AEG-1 3'-UTR and miR-499 mimic or miR-499 inhibitor for 48 hours. The expression of the AEG-1 mRNA (B) and protein (C) in HEPG2 cells were analyzed by real-time PCR and Western blot. D, Dual-luciferase reporter assay was performed in HEPG2 cells. * $P < .05$ versus Ct. HEPG2 cells were transfected with AEG-1 expression or shAEG-1 plasmid to construct stable AEG-1 overexpressing or knockdown cells. HEPG2 clone stably transfected with empty pcDNA3.1 (HEPG2-Ct) was used as a control. The effects of miR-499 on the stably overexpressing (E) or silencing (F) AEG-1 in the viability of HEPG2 cell by standard CCK-8 assay. G, The efficiency of AEG-1 overexpression and silence were confirmed by Western blot. Data represent mean \pm SD. *** $P < .001$. CCK-8 indicates cell counting kit-8; mRNA, messenger RNA; pcDNA, plasmid complementary DNA; PCR, polymerase chain reaction; SD, standard deviation; 3'-UTR, 3'-untranslated region.

of AEG-1 overexpression and silence in HEPG2 cells were confirmed by Western blot (Figure 4G). Taken together, these results indicate that miR-499 directly binds to AEG-1 3'-UTR and inhibits AEG-1 expression, and the effect of miR-499 targeting AEG-1 on cell proliferation. Thus, miR-499 may function as a negative regulator of the AEG-1 expression.

MicroRNA-499 Suppresses HCC Growth by Downregulation of AEG1

To investigate whether miR-499 exerts its antitumor effect through downregulating the activity of AEG-1, the real-time PCR was used to detect the mRNA expressions of AEG-1 in the adjacent nontumor and tumor tissues from patients with HCC.

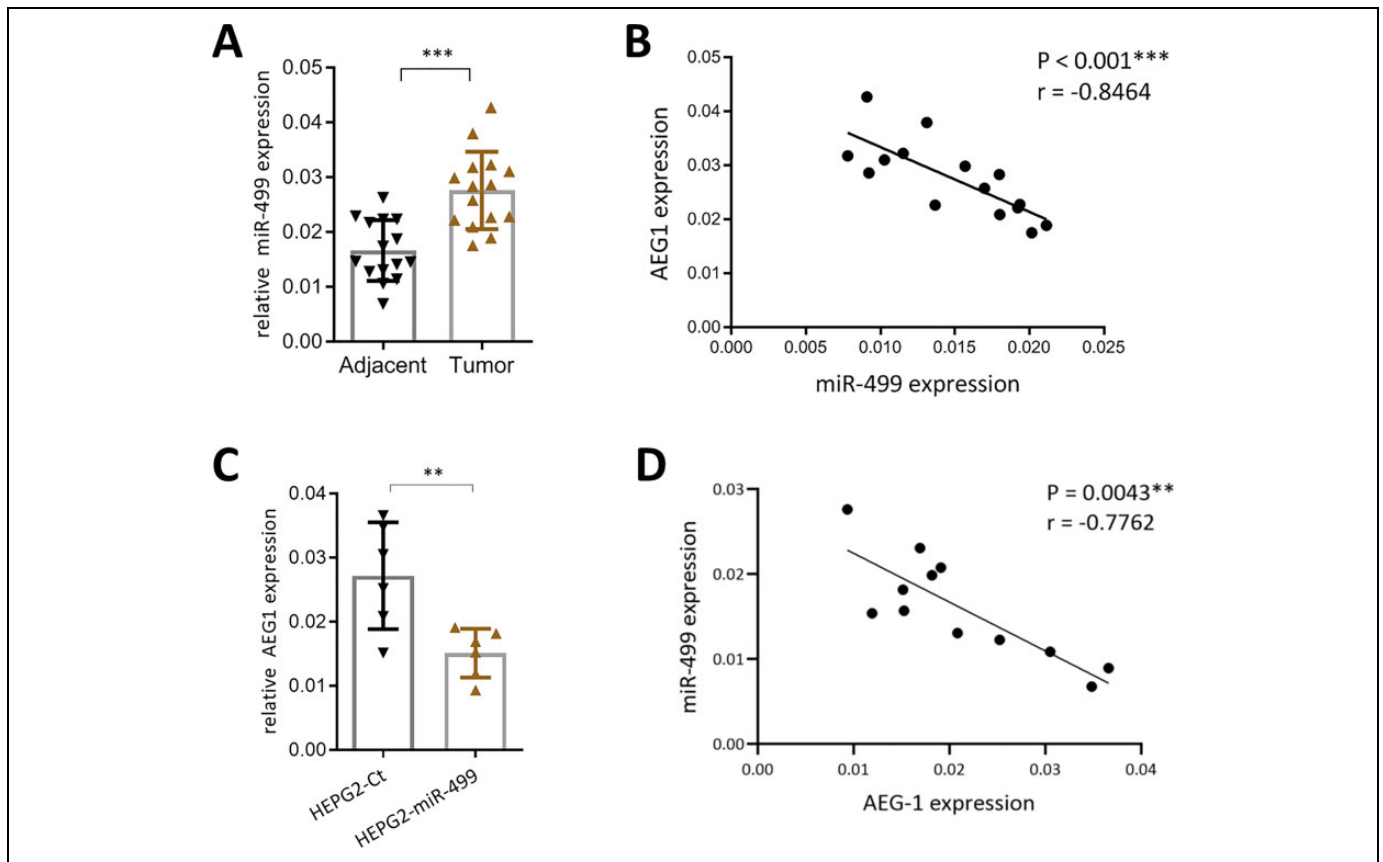


Figure 5. A, The expression of AEG-1 in human liver tumor and adjacent tissue was analyzed by real-time PCR. B, Spearman correlation test of microRNA-499 (miR-499) and AEG-1 mRNA expression in human tissues ($P < .001$). C, HEPG2 cells transfected with miR-499 or Ct vector were injected subcutaneously into nude mice, and real-time PCR was carried out to measure AEG-1 expression in nude mice tumorous liver specimens. $*P < .05$ compared with nontumorous specimens. D, correlation of the mRNA expressions of microRNA-499 and AEG-1 in nude mice as analyzed by Spearman rank correlation analysis; $*P < .001$ compared with the HEPG2-Ct group. AEG-1, astrocyte-elevated gene-1; mRNA, messenger RNA; PCR, polymerase chain reaction.

The results showed that compared with the normal group, the expression of AEG-1 in the tumor tissues was significantly increased while that of miR-499 was significantly decreased ($P < .05$; Figure 5A), which demonstrated that miR-499 closely correlated with AEG-1. Spearman's rank correlation analysis showed that mRNA expressions of miRNA-499 and AEG-1 were negatively correlated ($r = -0.8464$, $P < .001$; Figure 5B). As determined by real-time PCR, AEG-1 was significantly decreased in the liver tumor compared with paired non-tumor tissue mice specimens (Figure 5C). In addition, a statistically significant inverse correlation was revealed by Spearman correlation analysis between mRNA levels of miR-499 and AEG-1 in mouse tumor tissues ($r = -0.7762$; $P < .01$; Figure 5D).

Discussion

Hepatocellular carcinoma is considered as a refractory malignancy with a high mortality rate, and its global incidence has been increasing in recent years, especially in East Asia and Africa mainly due to the increasing incidence of hepatitis C

virus infection and chronic alcoholism.²⁵ The regular treatment approaches for HCC mainly include surgical resection, liver transplantation, chemoembolization, and radiotherapy, but the overall therapeutic efficacy is still unsatisfactory.²⁶ Therefore, how to make an early diagnosis and appropriate disease assessment of patients with HCC are the key to improve the survival rate and reduce the mortality rate. Recently, with the development of genomics and molecular biology, it has been found that the activation of proto-oncogenes and signaling pathways are closely linked to HCC progress.^{27,28} In our present work, we identified miR-499 as an antitumor miR in HCC using both *in vitro* experiments and *in vivo* HCC model, thus providing a candidate target for therapeutic intervention for HCC.

Previous studies showed that miR-449 acts as a tumor suppressor in prostate cancer through targeting CDK6 and CDC25A, thereby inhibiting pRb-E2F1 activity and inducing G1 phase cell cycle arrest.²⁹ Moreover, miR-499 was found to suppress HCC cell proliferation by targeting HDAC-1.¹⁸ In this study, we found that the expression of miR-499 in HCC tissues was lower than that in the adjacent noncancerous tissues. Downregulation of miR-499 in HEPG2 cells resulted in

significant suppression of HCC growth *in vivo* and *in vitro*. The results showed a new role for miR-499 in inhibiting tumor growth of HCC. This means miR-499 might serve as a novel diagnostic biomarker in patients with HCC. Besides, further studies are also needed to analyze the correlation between miR-499 expression and other pathological information of patients with HCC such as age, gender, alcohol history, tumor stage, metastasis, and survival, in order to ascertain whether miR-499 can also be used as a prognostic marker in HCC.

Subsequently, we predicted the target genes of miR-499 by online Targetscan software Human 7.2. Among these candidate target genes, AEG-1, also known as metadherin (MTDH),³⁰⁻³² was found to be the candidate target genes of miR-499. Astrocyte elevated gene-1 was identified as an oncogene in diverse types of cancers, including liver cancer.³³ The abnormally upregulated expression of AEG-1 in tumor cells often leads to the activation of several oncogenic signaling,³⁴ such as PI3K/Akt pathway.³⁵ Astrocyte elevated gene-1 deficiency nearly completely inhibited liver cancer development in mice,³⁶ suggesting a dominant role of AEG-1 in hepatocarcinogenesis. We confirmed miR-499 mimic can inhibit the expression of AEG-1 by real-time PCR and Western blot, and the luciferase activity of the miR-499-binding site of AEG-1 gene was significantly reduced after co-transfection with the miR-499 mimic in HEPG2 cells. Finally, an inverse correlation between miR-499 and AEG-1 expression in HCC confirmed that miR-499 suppresses HCC progression by downregulating AEG-1. Therefore, these results demonstrated that miR-499 plays tumor-suppressive roles in HCC progression by inhibiting AEG-1 expression. However, we cannot totally exclude the possibility that there are some other gene(s) responsible for the antitumor ability of miR-499, due to the fact that miRNAs typically have multiple mRNA targets. On the other hand, in the present work, we only employed a subcutaneous tumor model to investigate miR-499 function. Therefore, more HCC models such as a chemical-induced hepatic tumor or patient-derived xenograft model are needed to further evaluate the effect of miR-499 in the development of hepatocellular cancer.

Author Note

Jing Wang and Jia Li are the co-first authors.


Declaration of Conflicting Interests

The author(s) declared no potential conflicts of interest with respect to the research, authorship, and/or publication of this article.

Funding

The author(s) disclosed receipt of the following financial support for the research, authorship, and/or publication of this article: This work was supported by Shanghai Public Health Clinical Center.

ORCID iD

Jilin Cheng  <https://orcid.org/0000-0002-2059-7911>

References

1. Forner A, Llovet JM, Bruix J. Hepatocellular carcinoma. *Lancet*. 2012;379(9822):1245-1255.
2. McGlynn KA, London WT. The global epidemiology of hepatocellular carcinoma: present and future. *Clin Liver Dis*. 2011; 15(2):223-243.
3. Craig AJ, von Felden J, Lezana TG, Sarcognato S, Villanueva A. Tumour evolution in hepatocellular carcinoma. *Nat Rev Gastroenterol Hepatol*. 2020;17(3):139-152.
4. Yang JD, Hainaut P, Gores GJ, Amadou A, Plymoth A, Roberts LR. A global view of hepatocellular carcinoma: trends, risk, prevention and management. *Nat Rev Gastroenterol Hepatol*. 2019; 16(10):589-604.
5. Maluccio M, Covey A. Recent progress in understanding, diagnosing, and treating hepatocellular carcinoma. *CA Cancer J Clin*. 2012;62(6):394-399.
6. Siegel RL, Miller KD, Jemal A. Cancer statistics, 2015. *CA Cancer J Clin*. 2015;65(1):5-29.
7. Siegel RL, Miller KD, Jemal A. Cancer statistics, 2016. *CA Cancer J Clin*. 2016;66(1):7-30.
8. Lu ZL, Luo DZ, Wen JM. Expression and significance of tumor-related genes in HCC. *World J Gastroenterol*. 2005;11(25): 3850-3854.
9. Yates LA, Norbury CJ, Gilbert RJ. The long and short of microRNA. *Cell*. 2013;153(3):516-519.
10. Mohr AM, Mott JL. Overview of microRNA biology. *Semin Liver Dis*. 2015;35(1):3-11.
11. Kim D, Chang HR, Baek D. Rules for functional microRNA targeting. *BMB Rep*. 2017;50(11):554-559.
12. Winter J, Diederichs S. MicroRNA biogenesis and cancer. *Methods Mol Biol*. 2011;676:3-22.
13. Peng Y, Croce CM. The role of MicroRNAs in human cancer. *Signal Transduct Target Ther*. 2016;1:15004.
14. Bader AG, Brown D, Stoudemire J, Lammers P. Developing therapeutic microRNAs for cancer. *Gene Ther*. 2011;18(12): 1121-1126.
15. Calin GA, Croce CM. MicroRNA signatures in human cancers. *Nat Rev Cancer*. 2006;6(11):857-866.
16. Giordano S, Columbano A. MicroRNAs: new tools for diagnosis, prognosis, and therapy in hepatocellular carcinoma? *Hepatology*. 2013;57(2):840-847.
17. Wei W, Hu Z, Fu H, et al. MicroRNA-1 and microRNA-499 downregulate the expression of the ets1 proto-oncogene in HepG2 cells. *Oncol Rep*. 2012;28(2):701-716.
18. Buurman R, Gurlevik E, Schaffer V, et al. Histone deacetylases activate hepatocyte growth factor signaling by repressing microRNA-449 in hepatocellular carcinoma cells. *Gastroenterology*. 2012;143(3):811-820 e15.
19. Li J, Zhang N, Song LB, et al. Astrocyte elevated gene-1 is a novel prognostic marker for breast cancer progression and overall patient survival. *Clin Cancer Res*. 2008;14(11):3319-3326.
20. Tano K, Mizuno R, Okada T, et al. MALAT-1 enhances cell motility of lung adenocarcinoma cells by influencing the expression of motility-related genes. *FEBS Lett*. 2010;584(22): 4575-4580.

21. Yoo BK, Emdad L, Su ZZ, et al. Astrocyte elevated gene-1 regulates hepatocellular carcinoma development and progression. *J Clin Invest.* 2009;119(3):465-477.
22. Pandey MK, Sung B, Ahn KS, Kunnumakkara AB, Chaturvedi MM, Aggarwal BB. Gambogic acid, a novel ligand for transferrin receptor, potentiates TNF-induced apoptosis through modulation of the nuclear factor-kappaB signaling pathway. *Blood.* 2007;110(10):3517-3525.
23. Zhu K, Dai Z, Pan Q, et al. Metadherin promotes hepatocellular carcinoma metastasis through induction of epithelial-mesenchymal transition. *Clin Cancer Res.* 2011;17(23):7294-7302.
24. Jung HI, Ahn T, Bae SH, et al. Astrocyte elevated gene-1 overexpression in hepatocellular carcinoma: an independent prognostic factor. *Ann Surg Treat Res.* 2015;88(2):77-85.
25. El-Serag HB. Epidemiology of viral hepatitis and hepatocellular carcinoma. *Gastroenterology.* 2012;142(6):1264-1273. e1.
26. Couri T, Pillai A. Goals and targets for personalized therapy for HCC. *Hepatol Int.* 2019;13(2):125-137.
27. Yang N, Ekanem NR, Sakyi CA, Ray SD. Hepatocellular carcinoma and microRNA: new perspectives on therapeutics and diagnostics. *Adv Drug Deliv Rev.* 2015;81:62-74.
28. Negrini M, Gramantieri L, Sabbioni S, Croce CM. MicroRNA involvement in hepatocellular carcinoma. *Anticancer Agents Med Chem.* 2011;11(6):500-521.
29. Mao A, Liu Y, Wang Y, et al. miR-449a enhances radiosensitivity through modulating pRb/E2F1 in prostate cancer cells. *Tumour Biol.* 2016;37(4):4831-4840.
30. Li X, Kong X, Huo Q, et al. Metadherin enhances the invasiveness of breast cancer cells by inducing epithelial to mesenchymal transition. *Cancer Sci.* 2011;102(6):1151-1157.
31. He W, He S, Wang Z, et al. Astrocyte elevated gene-1(AEG-1) induces epithelial-mesenchymal transition in lung cancer through activating Wnt/beta-catenin signaling. *BMC Cancer.* 2015;15:107.
32. Sarkar D. AEG-1/MTDH/LYRIC in liver cancer. *Adv Cancer Res.* 2013;120:193-221.
33. Robertson CL, Srivastava J, Rajasekaran D, et al. The role of AEG-1 in the development of liver cancer. *Hepat Oncol.* 2015;2(3):303-312.
34. Huang Y, Li LP. Progress of cancer research on astrocyte elevated gene-1/Metadherin (Review). *Oncol Lett.* 2014;8(2):493-501.
35. Emdad L, Lee SG, Su ZZ, et al. Astrocyte elevated gene-1 (AEG-1) functions as an oncogene and regulates angiogenesis. *Proc Natl Acad Sci U S A.* 2009;106(50):21300-21305.
36. Robertson CL, Srivastava J, Siddiq A, et al. Genetic deletion of AEG-1 prevents hepatocarcinogenesis. *Cancer Res.* 2014;74(21):6184-6193.